Chemical Engineering Science 154 (2016) 42–53

Contents lists available at ScienceDirect

Chemical Engineering Science

journal homepage: www.elsevier.com/locate/ces

Online state of charge estimation of lithium-ion batteries: A moving horizon estimation approach

Jia-Ni Shen [a], Yi-Jun He [a,*], Zi-Feng Ma [a,b], Hong-Bin Luo [c], Zi-Feng Zhang [c]

[a] Dept. of Chemical Engineering, Shanghai Electrochemical Energy Devices Research Center, Shanghai Jiao Tong University, Shanghai 200240, China
[b] Sinopoly Battery Research Center, Shanghai 200241, China
[c] BYD Company Limited, Shenzhen 518118, China

HIGHLIGHTS

- A battery state-space model based MHE approach is proposed to SOC estimation.
- The convergence to true SOC of MHE is much faster than that of EKF.
- MHE is less sensitive to the poor initial SOC guess than EKF.
- MHE is a potential promising accurate and reliable approach for SOC estimation.

ARTICLE INFO

Article history:
Received 29 January 2016
Received in revised form
18 June 2016
Accepted 27 June 2016
Available online 28 June 2016

Keywords:
Lithium-ion batteries
State of charge
State-space model
Moving horizon estimation
Extended Kalman filter

ABSTRACT

Online state of charge (SOC) estimation of lithium-ion batteries (LIBs) relies not only on accurate battery model but also on effective state estimation method. In this study, a nonlinear battery state-space model based moving horizon estimation (MHE) approach is proposed to estimate SOC within the full range. The relationship between SOC and circuit parameters in battery model is captured by polynomial functions. The essential arrival cost in the MHE problem formulation is approximated by the filtering scheme and its covariance matrix is updated by extended Kalman filter (EKF) method. Hybrid pulse power characterization test is first used to guide battery model construction and tuning parameters determination in MHE. The constant current discharge test and dynamic stress test are then used to validate the applicability of the MHE and investigate the performance comparisons between MHE and EKF. The results demonstrate that compared to the EKF, the MHE is less sensitive to the poor initial SOC guesses and has faster convergence to the true SOC. The results thus validate that the MHE provides a potential promising approach to perform accurate, reliable and robust SOC estimation of LIBs.

1. Introduction

The lithium-ion batteries (LIBs), featured by high energy density, high power density, long cycle life and environmental friendliness, have gained tremendous attention from the past decade as one of the most prominent energy storage device and have been increasingly used in portable electronic devices, electric vehicles, smart grid, etc (Jongerden and Haverkort, 2009). The continuous improvements of positive and negative electrodes, separator and electrolyte performance as well as manufacture technology have made the LIBs more adaptable in various application fields (Hassoun and Scrosati, 2015). However, how to guarantee the safe, reliable and efficient operation of LIBs still remains a challenging task, which usually demands a properly designed battery management system (BMS) (Rezvanizaniani et al., 2014). In a BMS, state of charge (SOC) estimation is one of the key functions, which is helpful for protecting the battery from destructive operating regions such as overcharge and overdischarge (Cheng et al., 2011). However, as an internal parameter, SOC cannot be directly measured in LIBs but be inferred from other measured parameters or estimated in some way. Thus, various modeling and state estimation methods are proposed to describe the nonlinear relationship between SOC and measured parameters such as current (Fleischer et al., 2014), temperature (Erdinc et al., 2009) and cycle number (Miranda and Hong, 2013) and perform SOC estimation, respectively.

The SOC estimation methods can be broadly divided into three

* Corresponding author.
E-mail address: heyijun@sjtu.edu.cn (Y.-J. He).

http://dx.doi.org/10.1016/j.ces.2016.06.061
0009-2509/

categories: coulomb counting method (Ng et al., 2009), open circuit voltage (OCV) method (Lee et al., 2008; Xing et al., 2014) and model-based state estimation methods (Seaman et al., 2014). Although the coulomb counting method is the most common used one in real applications due to the simplicity, its performance is strongly dependent on the initial SOC guess and it significantly suffers from measurement error propagation without a feedback control. The OCV method estimates the SOC according to the predetermined relationship between OCV and SOC, which can be either a simple lookup table or a constructed analytical model. Because of a long rest time required to achieve a steady-state condition, the OCV method might be inefficient and impractical in real-time BMS application. In addition, the exhibition of voltage plateaus of LIBs would lead to the inaccurate SOC estimation. The model-based state estimation methods formalize the concept of filtering the measured voltage to estimate SOC and can be classified by means of modeling and state estimation techniques. The electrochemical model (Dey and Ayalew, 2014; Doyle et al., 1993), equivalent circuit model (ECM) (Chen and Rincon-Mora, 2006; Hu et al., 2012) and data-driven model (Chiasserini and Rao, 2001) are three types for modeling the dynamic behaviors of LIBs and are usually combined with Kalman filter (KF) based state estimation methods for performing SOC estimation. Although the electrochemical model can provide a detailed description of reaction and transport mechanisms in LIBs, the heavy computation cost limits its application in a real-time manner. In recent years, different model reduction techniques have been developed to reduce the computation time as well as maintain the accuracy of reduced model prediction. However, it should be noted that the parameters of reduced model are difficult to be efficiently determined for a commercial battery. Data-driven techniques such as fuzzy logic (Salkind et al., 1999) and artificial neural networks (Charkhgard and Farrokhi, 2010; Kang et al., 2014) have been adopted to establish the battery models using the measured input-output dataset without considering the inherent process mechanisms in LIBs. Although the data-driven approaches provide a universal approximator of the nonlinear dynamic behaviors in LIBs, the generalization performance cannot be guaranteed for unseen battery operating regions.

Compared to electrochemical and data-driven models, ECM can provide a good trade-off between model accuracy and complexity and has been widely used in BMS. Since the ECM is often nonlinear in nature, different KF based methods have been used to deal with the nonlinearities. The EKF is the first KF extension for nonlinear SOC estimation, in which the nonlinear ECM is linearized using Taylor expansion technique (Plett, 2004a, 2004b). Later, other nonlinear estimation methods, e.g. unscented Kalman filter (UKF) (He et al., 2013b; Sun et al., 2011), sigma-point Kalman filter (SPKF) (Plett, 2006) and particle filter (PF) (He et al., 2013c) have been introduced to further improve the accuracy and robustness of SOC estimation. The KF based methods require a proper initialization of SOC, otherwise, the SOC estimates will converge slowly to the true value even fail to converge (He et al., 2013b; Yang et al., 2016). However, the determination of initial SOC is usually a difficult task. In addition, the KF based methods lack constraint handling mechanism, which might lead to unreasonable SOC estimates, namely the estimated SOC might be greater than 1 or less than 0 (He et al., 2013a).

In last decades, moving horizon estimation (MHE) provides a powerful technique for state estimation of a nonlinear dynamic system (Rawlings and Ji, 2012). MHE is a multivariable estimation algorithm that mainly uses a dynamic model, a history of past measurements and an optimization cost function over the estimation horizon. Unlike the KF based methods, the MHE treats the state estimation problem as an optimization problem based on finite horizon measurements. The MHE has the advantages of the explicit consideration of state and parameter constraints, and the independence on specific error distribution (Rao et al., 2001; Rao et al., 2003). Moreover, it can provide fast convergence and reliable state estimates with a poor guess of the initial state (Haseltine and Rawlings, 2005). The MHE has attracted increasing attentions in chemical engineering community, such as distillation column (Findeisen et al., 2002; Kühl et al., 2011), polymerization reactor (Hedengren et al., 2007; Russo and Young, 1999) and low-density polyethylene tubular reactor (Zavala and Biegler, 2009). These applications of MHE in complex chemical processes have proven that the MHE is an effective solution for real-time state estimation. Recently, a few studies have applied the MHE to perform SOC estimation of LIBs based on the ECM (Ma et al., 2014; Pattel et al., 2014). The results show that the MHE can provide good SOC estimation performance at the millisecond level. However, the performance of MHE in these studies is only validated for a fairly narrow SOC range. The main reason is that the relationships between the circuit parameters and SOC are described by model-free lookup tables, which would make it difficult for directly performing SOC estimation within the normal operating range of 20–90% in LIBs. Hence, in this study, we employ a state-space model based on ECM, in which the relationship between circuit parameters and SOC is modeled using polynomial functions. The MHE is then used to perform SOC estimation based on the established state-space model. The proposed method will be verified by estimating SOC within a full range. A systematical performance comparison between the MHE and EKF is finally investigated for validating the robustness of the MHE in the condition of a poor guess of initial state within a large SOC range of LIBs.

The reminder of this paper is structured as follows. The battery state-space model for SOC estimation is first presented. Then, the basic principle of the MHE algorithm for SOC estimation is introduced. The effectiveness of the proposed method is then verified and validated by the experimental datasets and the performance comparison between the MHE and EKF is thoroughly investigated. Finally, conclusions are provided.

2. Battery model

As a model-based method, the accuracy and the efficiency of SOC estimation using MHE is strongly affected by the performance of battery model. A proper battery model for assisting in SOC estimation should not only be able to accurately capture the battery dynamic behaviors over a wide operating region, but also be simple enough to be integrated with online algorithms. ECM simulates the battery behaviors by using capacitors, voltage and current sources, and resistors from the view of circuit analysis. The number of resistance-capacitance (RC) parallel networks defined

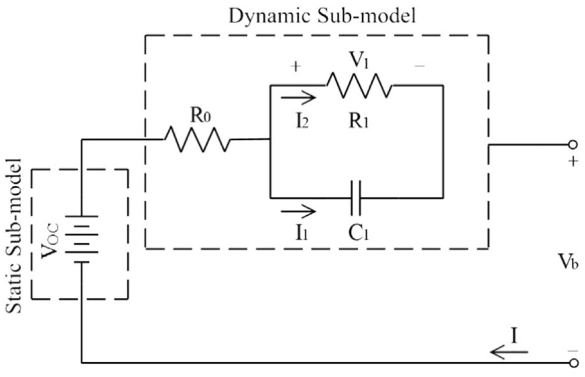

Fig. 1. 1-RC ECM for lithium battery.

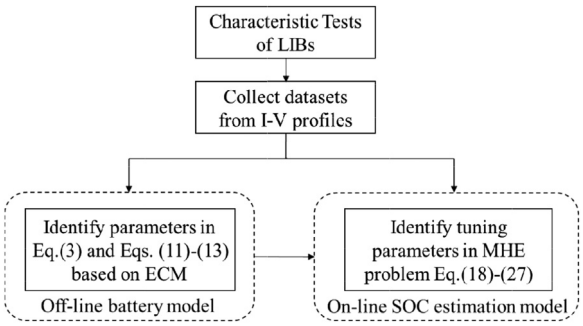

Fig. 2. The flowchart of MHE model construction for on-line SOC estimation.

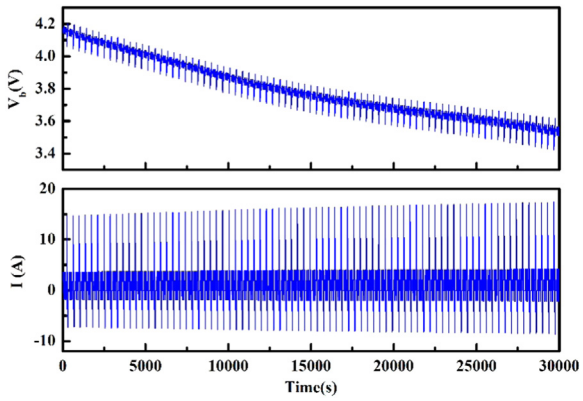

Fig. 4. The voltage and current profiles of DST.

as the order of ECM is the main effect on the model accuracy and the model complexity. In this work, we employ a first-order ECM model which has shown a good performance for the battery modeling in our previous woks (Shen et al., 2016). As shown in Fig. 1, ECM can be divided into three parts: a static sub-model, a dynamic sub-model and a load to produce charge or discharge regimes. A static sub-model used to obtain the OCV V_{OC} presents the effect of the thermodynamic properties of the battery chemistry on the battery voltage. A dynamic sub-model consisted of an ohmic resistance R_0 and a parallel RC network R_1C_1 presents the effect of the transient response on the battery voltage, which results from the changing load current. I is load current with a positive value at discharging and a negative value at charging. In general, these circuit parameters V_{OC}, R_0, R_1 and C_1 are dependent on SOC and temperature. In this study, we only focus our attention on a specific constant temperature for verifying the effectiveness of the MHE based SOC estimation method.

SOC over time t can be calculated by coulomb counting.

$$SOC_t = SOC_0 - \frac{1}{C_n}\int_0^t I_\tau d\tau \tag{1}$$

where SOC_0 is the initial value of SOC and C_n is the nominal capacity of battery. Since current and voltage are often measured at discrete time with a specific sampling frequency, the integration of the right-hand second term of Eq. (1) can be easily calculated by summation and then Eq. (1) is reformulated as

$$SOC_{k+1} = SOC_k - \frac{I_k \Delta t}{C_n} \tag{2}$$

where SOC_k denotes the value of SOC at discrete times t_k, and Δt is the sampling interval.

In the part of static sub-model, a monotone polynomial OCV model developed in our previous work (He et al., 2015) is used to determine the relationship between the OCV and SOC,

$$V_{OC}(SOC) = \sum_{j=0}^{M} \alpha_j SOC^j \tag{3}$$

where α_j are the polynomial coefficient and M is the polynomial order.

In the part of dynamic sub-model, based on Kirchhoff's current law, the relationship between currents can be described as

$$I = I_1 + I_2 \tag{4}$$

where I_1 and I_2 are the currents through resistance R_1 and capacitance C_1, respectively. Based on further electric circuit analysis, the relationship between currents, voltage and capacitance can be obtained as

$$I_1 = C_1 \frac{dV_1}{dt} \tag{5}$$

$$I_2 = \frac{V_1}{R_1} \tag{6}$$

From (Eqs. (4)–(6), the voltage V_1 can be derived as

$$\frac{dV_1}{dt} = \frac{I}{C_1} - \frac{V_1}{C_1 R_1} \tag{7}$$

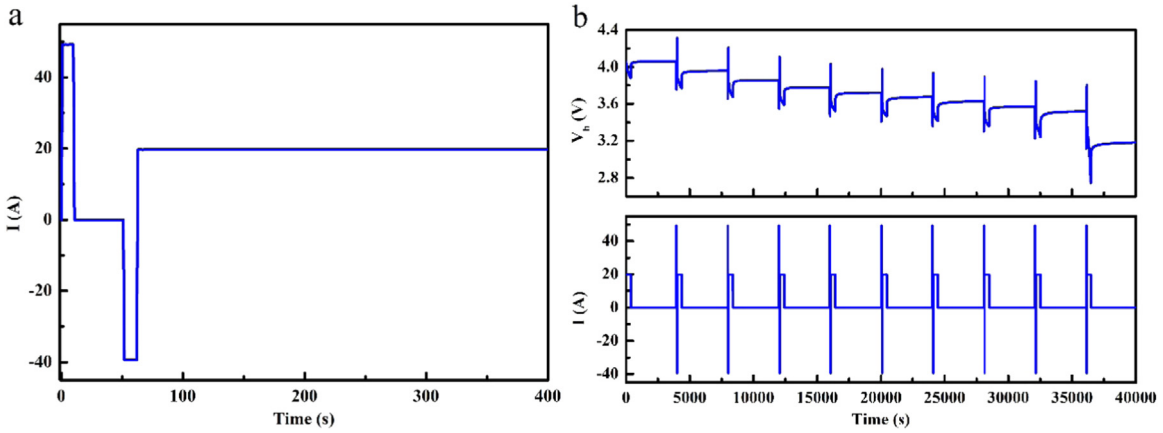

Fig. 3. HPPC test (a) One HPPC cycle followed by 1 C rate discharge and (b) A complete HPPC test profiles.

Table 1
Polynomial relationship between SOC and circuit parameters of ECM.

Circuit parameters	Polynomial forms
V_{oc}	$485.76SOC^{11}-2044.70SOC^{10}+3000.00SOC^{9}-934.20SOC^{8}-2309.12SOC^{7}+3000.00SOC^{6}-1426.11SOC^{5}+148.51SOC^{4}+125.72SOC^{3}-53.31SOC^{2}+8.58SOC+3.04$
R_0	$0.065SOC^{5}-0.192SOC^{4}+0.215SOC^{3}-0.109SOC^{2}+0.022SOC+0.005$
R_1	$-0.396SOC^{5}+1.114SOC^{4}-1.180SOC^{3}+0.576SOC^{2}-0.128SOC+0.015$
C_1	$-40000.00SOC^{5}+1317.82SOC^{4}+40000.00SOC^{3}-40000.006SOC^{2}+19422.74SOC+12199.92$

Table 2
The effect of horizon length on SOC estimation accuracy and the average computing time for one estimation in the HPPC profile.

Horizon length	10	20	30	40
RMSE	11.94%	0.47%	0.59%	0.57%
Computing time/s	0.23	0.57	0.69	0.96

The battery terminal voltage depending on two sub-models can be then written as

$$V_b = V_{OC}(SOC) - V_1 - IR_0 \tag{8}$$

Hence, the complete model for describing the nonlinear dynamics of the LIBs is obtained. To perform parameter estimation efficiently and improve the speed of state estimation, the analytical solution of the voltage V_1 in Eq. (7) is calculated. At the time interval $[t_{k-1}, t_k]$, we suppose that the circuit parameters, i.e. R_1 and C_1, keep constant and denote them as $R_{1,\,k-1}$ and $C_{1,\,k-1}$, respectively. Then, at discrete time t_k, the voltage $V_{1,k}$ can be analytically derived from Eq. (7) as

$$V_{1,k} = V_{1,k-1}\exp\left(-\frac{\Delta t}{\tau_{1,k-1}}\right) + I_{k-1}R_{1,k-1}\left[1-\exp\left(-\frac{\Delta t}{\tau_{1,k-1}}\right)\right] \tag{9}$$

where $\tau_{1,k} = R_{1,k-1}C_{1,k-1}$ denotes the time constant of the parallel RC network during the time interval $[t_{k-1}, t_k]$. Then, the terminal voltage $V_{b,k}$ in Eq. (8) at discrete time t_k can be represented as

$$V_{b,k} = V_{OC}(SOC_k) - V_{1,k} - I_k R_{0,k} \tag{10}$$

The above time-varying circuit parameters can be represented as polynomial functions of SOC and described as

$$R_{0,k} = R_0(SOC_k) = \sum_{j=0}^{N}\beta_{1,j}SOC_k{}^j \tag{11}$$

$$R_{1,k} = R_1(SOC_k) = \sum_{j=0}^{N}\beta_{2,j}SOC_k{}^j \tag{12}$$

$$C_{1,k} = C_1(SOC_k) = \sum_{j=0}^{N}\beta_{3,j}SOC_k{}^j \tag{13}$$

where $\beta_{1,j}$, $\beta_{2,j}$ and $\beta_{3,j}$ are the polynomial coefficients and N is the polynomial order. In this study, a least-square minimization problem is constructed and then solved to estimate these polynomial coefficients by means of the battery testing dataset.

Based on the ECM described in Eqs. (2) and (9)–(13), the dynamic behaviors of LIBs can be further expressed in the standard discrete time state-space model as

$$\mathbf{x}_{k+1} = \mathbf{F}(\mathbf{x}_k, u_k) + \mathbf{w}_k \tag{14}$$

$$y_k = h(\mathbf{x}_k, u_k) + v_k \tag{15}$$

where $\boldsymbol{x}_k = \left[SOC_k, V_{1,k}\right]^{\mathrm{T}}$ is the state vector at time t_k, $u_k = I_k$ is the system input at time t_k, $y_k = V_{b,k}$ is the system measurement at time t_k, $\mathbf{w}_k$ is the state normal distribution noise with zero mean and covariance $\boldsymbol{Q}_k$, and v_k is measurement normal distribution noise with zero mean and variance R_k. The functions of $\boldsymbol{F}(\boldsymbol{x}_k,u_k)$ and $h(\boldsymbol{x}_k,u_k)$ are expressed as Eqs. (16) and (17) respectively.

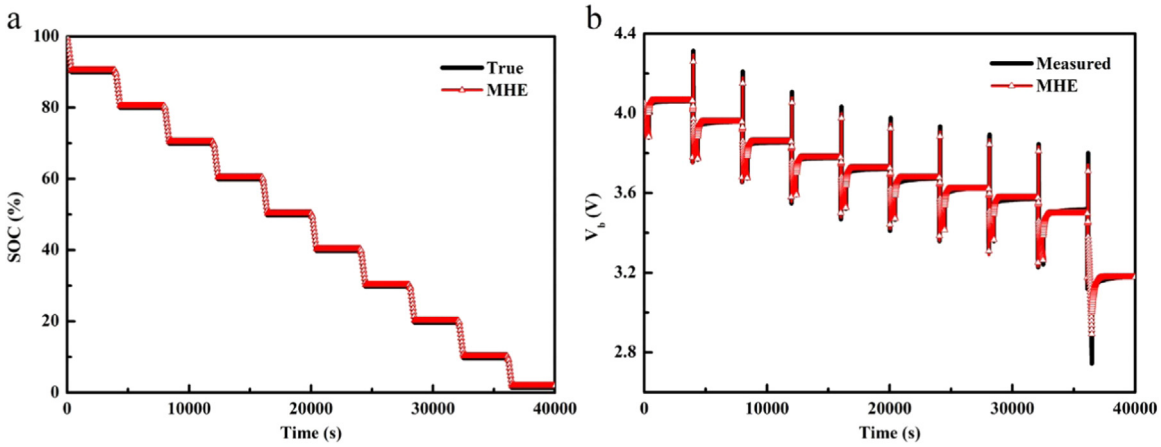

Fig. 5. Estimation results and experimental values for the HPPC test. (a) SOC and (b) battery terminal voltage.

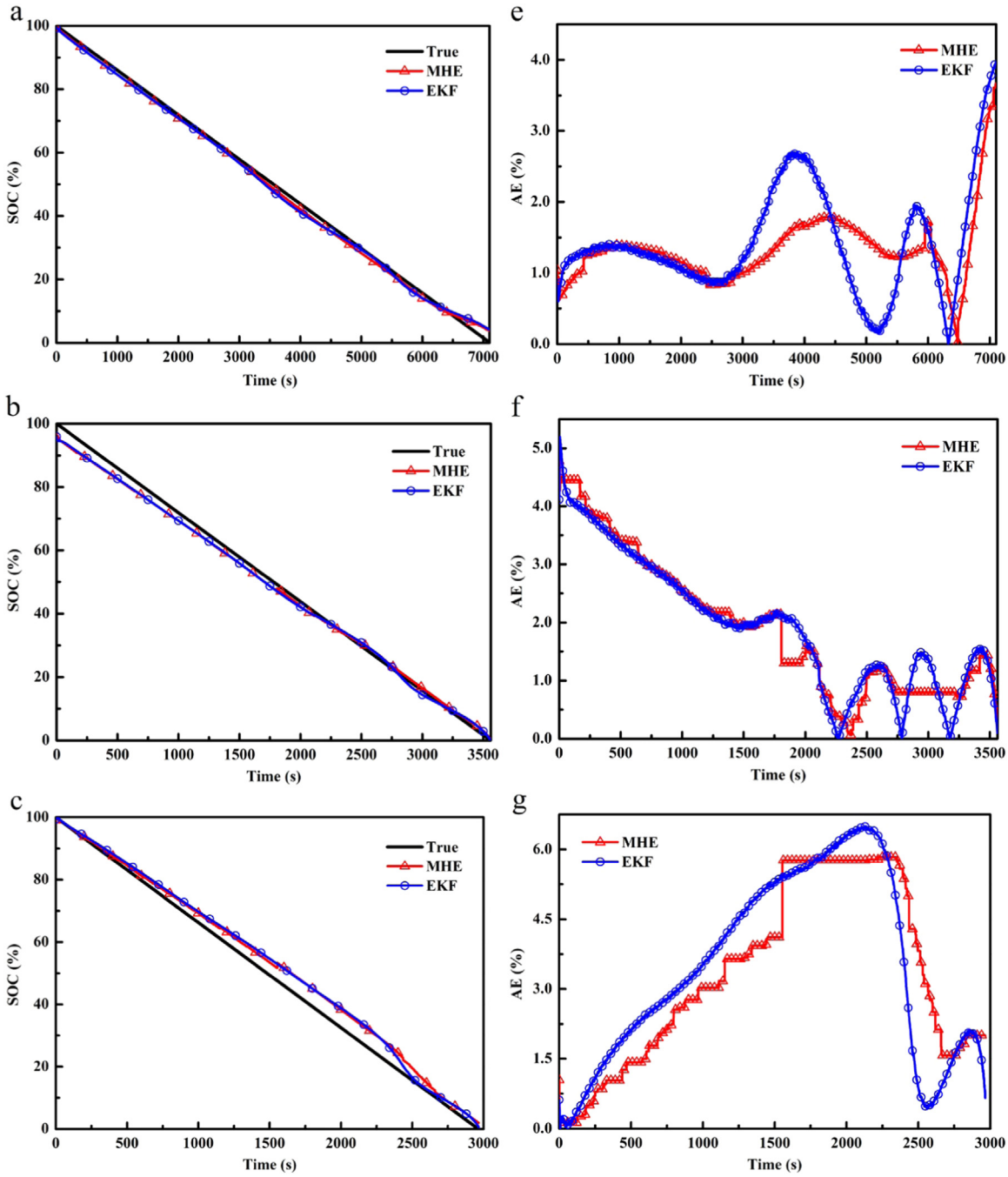

Fig. 6. SOC estimation and AE profiles of MHE and EKF with the correct initial SOC guess for three CCDT profiles in whole SOC range: (a) and (d) 0.5C-rate; (b) and (e) 1C-rate; (c) and (f) 1.2C-rate.

Table 3
The RMSE comparison between MHE and EKF with the correct initial guesses for three CCDT profiles in the whole SOC range.

	0.5C-rate	1C-rate	1.2C-rate
MHE	0.99%	2.26%	3.80%
EKF	1.72%	2.24%	3.98%

$$\boldsymbol{F}(\boldsymbol{x}_k, u_k) = \begin{bmatrix} SOC_k - \dfrac{I_k \Delta t}{C_n} \\ V_{1,k}\exp\left(-\dfrac{\Delta t}{\tau_1(SOC_k)}\right) + I_k R_1(SOC_k)\left[1 - \exp\left(-\dfrac{\Delta t}{\tau_1(SOC_k)}\right)\right] \end{bmatrix} \tag{16}$$

$$h(\mathbf{x}_k, u_k) = V_{OC}(SOC_k) - V_{1,k} - I_k R_0(SOC_k) \tag{17}$$

Because the battery state-space model described above is nonlinear in nature, it requires nonlinear state estimation methods such as EKF and MHE to estimate SOC. Note that since most of state estimation techniques are classified into probabilistic approaches, both the state and measurement variables are simply assumed to be subjected to additive random disturbances as shown in Eqs. (14) and (15).

3. Moving horizon estimation

From a viewpoint of Bayesian theory, the nonlinear constrained state estimation problem can be formulated as a full information

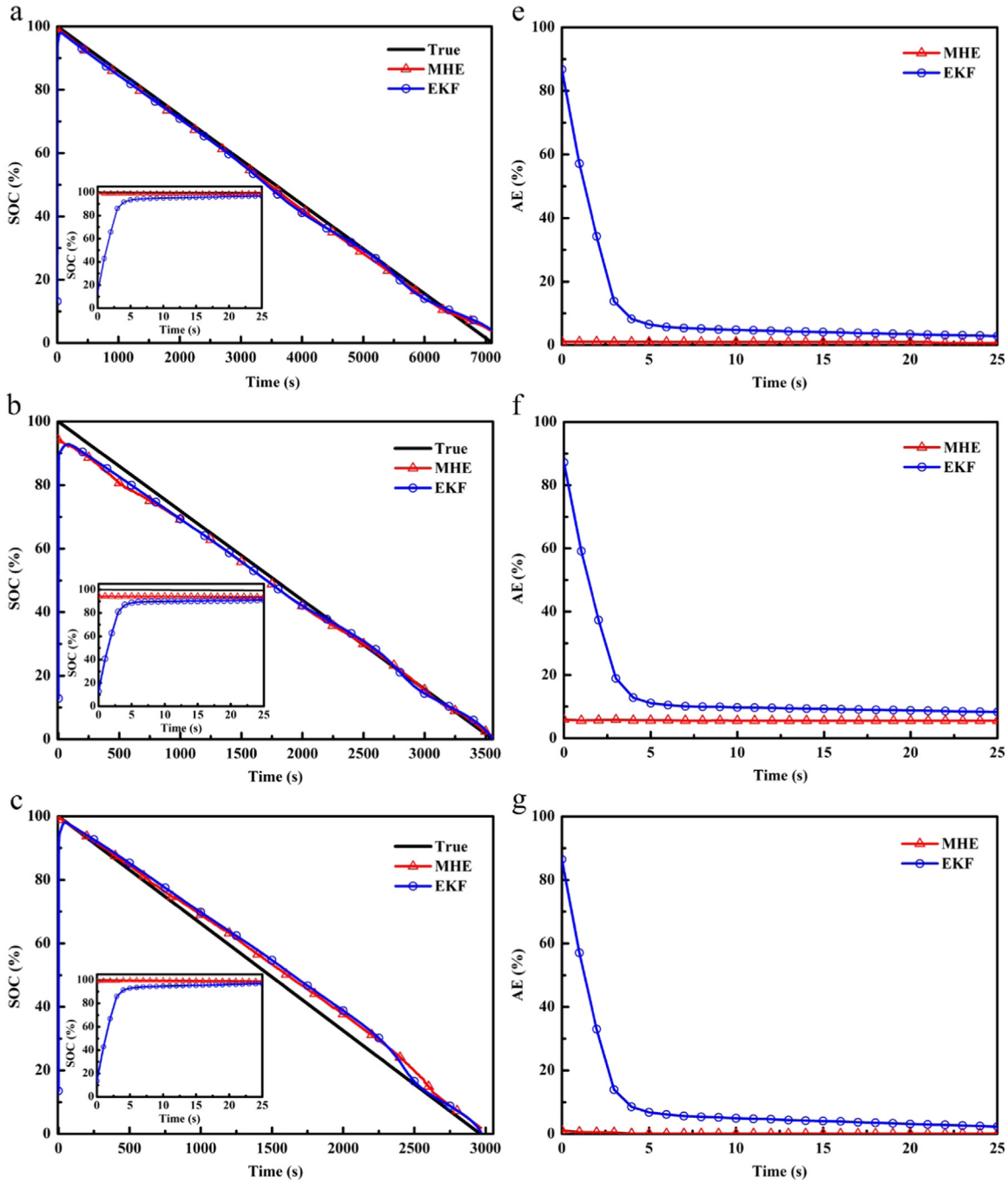

Fig. 7. SOC estimation and AE profiles of MHE and EKF with the initial SOC guess value of 0% for the first 25 s of three CCDT profiles: (a) and (d) 0.5C-rate; (b) and (e) 1C-rate; (c) and (f) 1.2C-rate.

estimation (FIE) problem (Rao et al., 2003). However, since the size of the FIE problem increases with the increasing of measurements, the direct online implementation of FIE is often computational infeasible. To overcome this computational problem, the MHE is proposed to transfer the FIE problem into a finite horizon optimization problem and solves this nonlinear optimization problem online repeatedly.

Assume that the battery is currently operated at time t_k and the most recent L input measurements $\{I_{k-L+1},\ldots,I_k\}$ and output measurements $\{V_{b,k-L+1},\ldots,V_{b,k}\}$ at time $\{t_{k-L+1},\ldots,t_k\}$ are available to determine the current state of the battery $\boldsymbol{x}_k$. The MHE problem at time t_k with horizon of L for SOC estimation can be completely formulated as the following constrained least-squares optimization problem,

$$\min_{\boldsymbol{x}_{k-L+1},\ldots,\boldsymbol{x}_k} \theta(\boldsymbol{\rho}) + \sum_{i=k-L+1}^{k-1} \|\mathbf{w}_i\|^2_{Q^{-1}} + \sum_{i=k-L+1}^{k} \|v_i\|^2_{R^{-1}} \tag{18}$$

s.t.

$$\mathbf{x}_{k-L+1} = \bar{\mathbf{x}}_{k-L+1} + \boldsymbol{\rho} \tag{19}$$

$$\begin{bmatrix} SOC_{i+1} \\ V_{1,i+1} \end{bmatrix} = \begin{bmatrix} SOC_i - \dfrac{I_i \Delta t}{C_n} \\ V_{1,i}\exp\left(-\dfrac{\Delta t}{\tau_1(SOC_i)}\right) + I_i R_1(SOC_i)\left[1 - \exp\left(-\dfrac{\Delta t}{\tau_1(SOC_i)}\right)\right] \end{bmatrix} + \begin{bmatrix} w_{1,i} \\ w_{2,i} \end{bmatrix}$$
$$i = k-L+1, \cdots, k-1 \tag{20}$$

$$V_{b,i} = V_{OC}(SOC_i) - V_{1,i} - I_k R_0(SOC_i) + v_i, \quad i = k-L+1, \cdots, k \tag{21}$$

$$V_{OC}(SOC_i) = \sum_{j=0}^{M} \alpha_j SOC_i^j, \ i = k-L+1, \cdots, k \tag{22}$$

$$R_0(SOC_i) = \sum_{j=0}^{N} \beta_{1,j} SOC_i^j, \ i = k-L+1, \cdots, k \tag{23}$$

$$R_1(SOC_i) = \sum_{j=0}^{N} \beta_{2,j} SOC_i^j, \ i = k-L+1, \cdots, k-1 \tag{24}$$

$$C_1(SOC_i) = \sum_{j=0}^{N} \beta_{3,j} SOC_i^j, \ i = k-L+1, \cdots, k-1 \tag{25}$$

$$\tau_1(SOC_i) = R_1(SOC_i)C_1(SOC_i), \ i = k-L+1, \cdots, k-1 \tag{26}$$

$$0 \le SOC_i \le 1, \ \ i = k-L+1, \cdots, k \tag{27}$$

where $\bar{\mathbf{x}}_{k-L+1}$ is the prior estimate of the initial state at time t_{k-L+1} given all of the measurements y_k from time t_0 to t_{k-L} and $\boldsymbol{\rho}$ denotes the error in the initial estimate. The first term $\theta(\boldsymbol{\rho})$ in the objective function is typically called the arrival cost, which summarizes past measurement information before time t_{k-L+1}. The arrival cost in the filtering scheme (Rao et al., 2001) is usually defined as

$$\theta(\boldsymbol{\rho}) = \|\boldsymbol{\rho}\|^2_{P^{-1}} \tag{28}$$

Note that P, Q and R are positive definite weighting matrices to penalize the deviations of initial estimate, the battery dynamic model and output model respectively. In general, P, Q and R are initially defined as diagonal matrices by the user. Both covariance matrices Q and R are usually set constant during the state estimation procedure, while covariance matrix P is often updated using the EKF method (Rao et al., 2003) for the nonlinear state estimation problem and shown as

$$P_{i+1} = B_i Q_i B_i^{\mathrm{T}} + A_i(P_i - P_i C^{\mathrm{T}}(R + C_i P_i C_i^{\mathrm{T}})^{-1} C_i P_i) A_i^{\mathrm{T}} \tag{29}$$

where A_i and B_i are the Jacobian matrices of state function with respect to state variables and noises respectively, and C_i is the Jacobian matrix of measurement function with respect to state variables.

In addition, based on the definition of SOC, the lower and upper bounds of SOC should be 0 and 1 respectively. Since most of recursive estimation methods such EKF and UKF cannot explicitly handle such constraint, the estimated SOC might be lower than 0 or greater than 1. However, in the MHE formulation, it is easy to handle this SOC constraint shown in Eq. (27).

Based on the above descriptions, the flowchart of MHE model construction for on-line SOC estimation can be depicted in Fig. 2. The off-line battery model based on 1-RC ECM is first established, and then the on-line SOC estimation model is produced by integrating the off-line model with MHE algorithms. Both off-line model construction and online SOC estimation are carried out by means of the datasets from voltage response curve of LIBs.

Two criteria, i.e. the root mean square error (RMSE) and absolute error (AE), are used to evaluate the SOC estimation performance and are defined as follows, where $\hat{SOC}_i$ is the estimate value of SOC_i

$$\mathrm{RMSE} = \sqrt{\frac{\sum_{i=1}^{k} \left|\hat{SOC}_i - SOC_i\right|^2}{k}} \tag{30}$$

$$\mathrm{AE}_i = \left|\hat{SOC}_i - SOC_i\right| \tag{31}$$

Table 4
The RMSE comparison between MHE and EKF with the correct and the extreme poor initial SOC guesses for the first 25 s of three CCDT profiles.

	0.5C-rate		1C-rate		1.2C-rate	
	MHE	EKF	MHE	EKF	MHE	EKF
SOC_0=100%	0.92%	0.67%	4.50%	4.94%	0.32%	0.25%
SOC_0=0%	1.00%	22.45%	5.57%	24.30%	0.38%	22.34%

4. Experimental

A commercial SINOPOLY SP-60155229 NMC cathode Lithium-ion battery with nominal capacity of 20 Ah and nominal voltage of 3.6 V

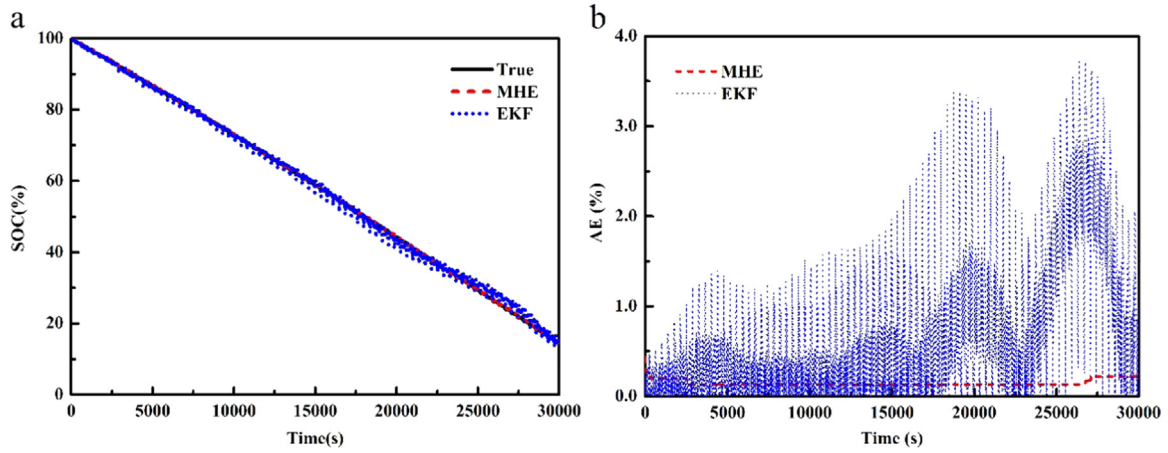

Fig. 8. Estimation results of MHE and EKF with the correct initial SOC guess for the DST profile in 10–100% SOC range: (a) SOC estimation profiles and (b) AE profiles.

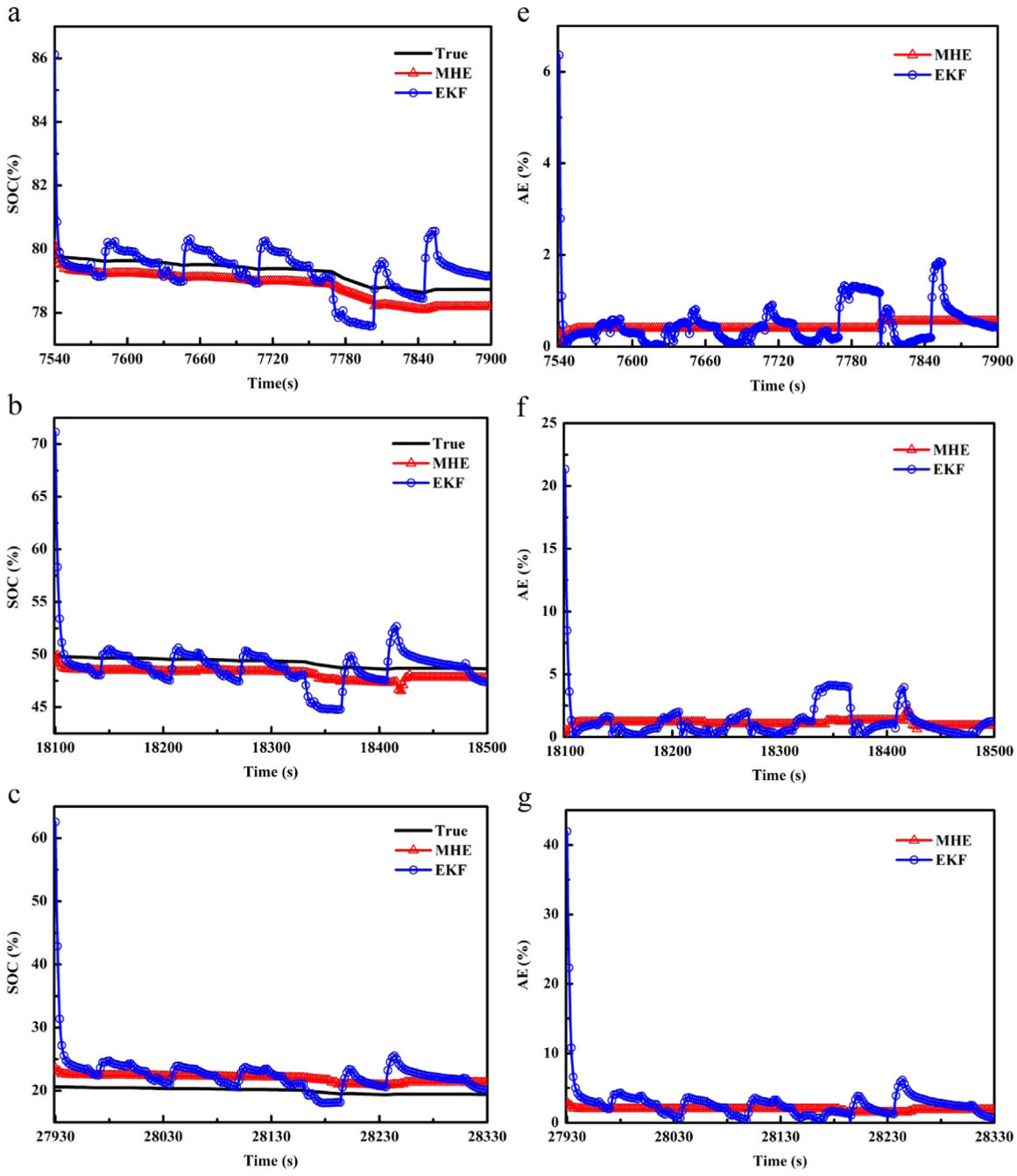

Fig. 9. SOC estimation and AE profiles of MHE and EKF with the initial SOC guess of 100% for DST cycles with different initial SOC: (a) and (d) 80% SOC; (b) and (e) 50% SOC; (c) and (f) 20% SOC.

was used to test the battery dynamic behaviors at 293 K, which were conducted with a NEWARE CT-3002-5V500A battery test system and a HARDY HLT4005P programmable temperature test chamber. The data acquisition system has a logging frequency of 1 Hz, and the measurement precision of both current and voltage is 0.05%. The battery was first charged to its full capacity through constant current constant voltage, and then rested for 2 h. Then, three characteristic tests, i.e. hybrid pulse power characterization (HPPC) test (Hunt, 2003), constant current discharge test (CCDT) and dynamic stress test (DST) (Hunt, 1996) were performed.

The HPPC test is conducted to construct battery model. As shown in Fig. 3(a), a HPPC current profile consists of a 10 s discharge of 2.5 C rate (50 A), a 40 s rest and a 10 s charge of 2 C rate (40 A). A subsequent 1 C rate is used to discharge the battery to a particular SOC. The voltage response curve during a complete HPPC test is shown in Fig. 3(b). The battery was first discharged at 1 C rate for 360 s to reduce 10% of SOC and then rested for 3600 s. Then, the profile in Fig. 3(a) was repeated conducted until to 0% SOC, separated by a 3600 s rest period.

Both CCDT and DST are conducted to validate the SOC estimation performance of MHE approach. In the CCDTs, three discharge rates, i.e. 0.5 C, 1 C and 1.2 C, are used to investigate the effect of discharge currents on SOC estimation. All three CCDTs were conducted to discharge the battery from 100% to 0% SOC. The DST which consists of charge, discharge and rest modes is used as the variable power discharge test and is conducted to discharge the battery from 100% to 10% SOC. The battery discharge voltage response curve corresponding to a repeated DST sequence with no time delay is shown in Fig. 4.

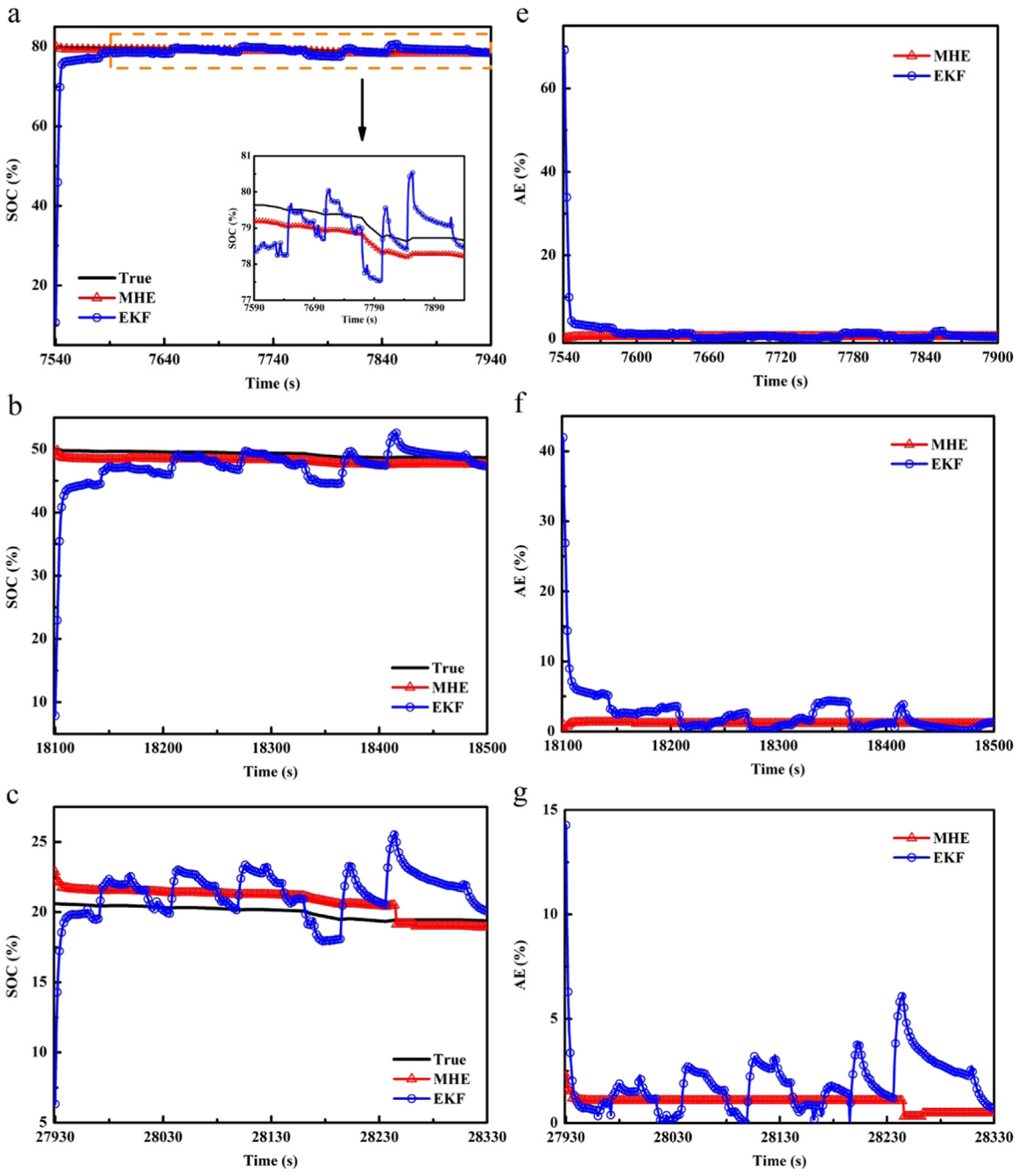

Fig. 10. SOC estimation and AE profiles of MHE and EKF with the initial SOC guess of 0% for DST cycles with different initial SOC: (a) and (d) 80% SOC; (b) and (e) 50% SOC; (c) and (f) 20% SOC.

Table 5
The RMSE comparison between MHE and EKF with two extreme poor initial SOC guesses for different DST cycles.

	80% SOC		50% SOC		20% SOC	
	MHE	EKF	MHE	EKF	MHE	EKF
$SOC_0=100\%$	0.44%	0.71%	1.14%	2.15%	1.88%	4.20%
$SOC_0=0\%$	0.44%	5.12%	1.15%	4.45%	1.03%	2.36%

5. Results and discussion

The datasets collected from HPPC test at 293 K are first used to identify the battery state-space model and optimally determine the tuning parameters in MHE. Then, the datasets from CCDT and DST at 293 K are used to thoroughly investigate SOC estimation performance comparison between MHE and EKF. Both MHE and EKF are implemented in MATLAB with model predictive control tools package and the nonlinear optimization problem of MHE is solved by interior-point algorithm (Amrit and Rawlings, 2008). All computations are carried out on a PC with 2.40 GHz processor and 8 GB of RAM.

5.1. Battery model identification and MHE parameters tuning

Before implementing online SOC estimation, the battery model parameters, i.e. polynomial coefficients of circuit parameters, are first identified based on the experimental data form HPPC test.

Table 1 lists the estimated polynomial functions of V_{oc}, R_0, R_1 and C_1. The RMSE value of the terminal voltage for this HPPC profile is less than 10 mV. The detailed parameter estimation procedure and a thorough performance evaluation of the constructed off-line model is out of scope in this study, a more detailed discussion can be referred to our previous work (Shen et al., 2016).

Based on the constructed battery model, the effects of tuning parameters on the SOC estimation performance in MHE are next investigated. The tuning parameters in MHE include the covariance matrices and horizon length. To obtain the covariance matrices, we first make rough assumptions on a realistic magnitude of state noises and then finely tune the matrices to achieve a satisfying SOC estimation performance. The finally used matrices are: the initial parameter covariance matrix $P=\mathrm{diag}(1000\ 1)$, the state noise covariance matrix $Q=\mathrm{diag}(0.1\ 0.01)$, and the measurement noise covariance matrix $R=0.01$. Table 2 shows the effect of horizon length on SOC estimation accuracy and the average computing time for one estimation. The RMSE value significantly decreases from 11.94% to 1.30% as the horizon length increases from 10 to 20. When the horizon length increases from 20 to 30, the RMSE value is decreased to 0.59%. Further increase the horizon length from 30 to 40, the RMSE value keeps almost the same. Although a long horizon length could improve the SOC estimation accuracy, it would result in a high computational cost in MHE. Hence, in this study, a horizon length of 30 is selected to balance the trade-off between the SOC estimation accuracy and computational cost. Note that the optimal tuned horizon length is relatively long when compared to this small dynamic model with only two state variables. That might result from the complex dynamic behaviors in LIBs described by the RC branch.

Based on the obtained optimal parameters, the MHE estimation results and the experimental values for the whole HPPC profile are plotted in Fig. 5. It is observed that the estimated SOC and filtered terminal voltage almost coincide with the true SOC and measured voltage respectively. It indicates that the constructed battery model can describe the complex dynamic behaviors well and the optimal tuning parameters are ready for implementing the SOC estimation in other operating conditions.

5.2. MHE performance for SOC estimation

In this section, the MHE approach with the above optimal tuning parameters is applied to the SOC estimation for both CCDT and DST profiles. The estimation results are compared to those obtained by the EKF. To ensure a fair comparison, the tuning parameters in the EKF are optimally determined by means of the HPPC dataset. The covariance matrices used in the EKF are: $P=\mathrm{diag}(100\ 1)$, $Q=\mathrm{diag}(10\ 0.01)$ and $R=10$. Since the initial SOC is difficult to be accurately determined in real applications, besides the correct initial SOC guess, two extreme poor initial SOC guesses, i.e. 100% and 0%, will be also used in both MHE and EKF to investigate whether they can converge to the true SOC and how fast they can converge to the true SOC.

5.2.1. CCDT case

For the 0.5C-, 1C- and 1.2C-rate CCDT profiles in the whole SOC range, the estimation results based on the MHE and EKF with the correct initial SOC guess are compared in Fig. 6(a), (b) and (c) respectively, and the corresponding AE profiles are shown in Fig. 6(d), (e) and (f) respectively. It can be observed from Fig. 6 that both MHE and EKF show the similar performance for these three CCDT profiles. The SOC estimation errors generally keep considerable small except at low SOC range in 0.5C-rate CCDT profile, high SOC range in 1C-rate CCDT profile and medium SOC range in 1.2C-rate CCDT profile. The relatively large SOC estimation error in those regions is possibly caused by the model mismatch, as the parameters of battery model are estimated from a HPPC profile without any information about long-time continued discharge dynamics. Hence, if some CCDT datasets are introduced to guide the battery model construction, the SOC estimation accuracy would be improved. Additionally, since MHE is in nature able to handle with simultaneous state and parameter estimation problem, it is possible to improve the SOC estimation accuracy by establishing the augmented state-space model with circuit parameters. From Fig. 6(d)–(f), the maximum AE values of MHE and EKF are below 4%, 5.5% and 6.5% for the 0.5C-, 1C- and 1.2C-rate CCDT profiles, respectively. Table 3 shows the RMSE comparison between MHE and EKF with the correct initial guess for three CCDT profiles in the whole SOC range. From Table 3, it is found that the RMSE of 0.99% in MHE is slightly smaller than that of 1.72% in EKF for the 0.5C-rate CCDT profile, while for the 1C- and 1.2C-rate CCDT profiles, the RMSE values of MHE and EKF are quite close. These performance comparison results illustrate that the SOC estimation accuracy of MHE and EKF is almost comparable for these three CCDT profiles. Hence, in the case of SOC estimation with the correct initial SOC guess, it seems to be favor to select the computational efficient EKF method. However, before selecting the most suitable SOC estimation method, more performance evaluation should be investigated under the conditions of SOC estimation with the poor initial state guess or other battery operating profiles.

To evaluate whether the MHE and EKF are sensitive to the initial guess of SOC, an extreme poor initial SOC guess of 0% is used in both MHE and EKF for three CCDT profiles. Fig. 7(a)–(c) shows the comparisons of estimation profiles between the MHE and EKF with the initial SOC guess of 0%. It is clearly found that the MHE converges to the true SOC much faster than the EKF at first, and then they perform equally well. From an enlarged look at first 25 s, it could be observed that the MHE takes only one second to recover from the poor initial SOC guess, while the EKF usually takes more than five seconds. That is also verified by the AE profiles of SOC estimation shown in Fig. 7(d)–(f). It is found that the first AE values of MHE have been decreased to a very small level, i.e. 1.04%, 5.81% and 1.12% for the 0.5C-, 1C- and 1.2C-rate CCDT profiles respectively, while that of EKF are larger than 80% for these three CCDT profiles. Table 4 shows the RMSE comparison of MHE and EKF with the correct and extreme poor initial SOC guesses for the first 25 s of three CCDT profiles. It is observed that the RMSE values of MHE with the extreme poor initial SOC guess is almost the same as that with the correct initial SOC guess for all three CCDT profiles, while the RMSE values of EKF with the extreme poor initial SOC guess is more than five times of that with the correct initial SOC guess for all three CCDT profiles. It is due to the fact that, EKF method which only utilizes current observation in the update cannot acquire the sufficient information, resulting in the ineffective estimate of the states, while the MHE can make use of previous and current measurements in one estimation. These results demonstrate a faster convergence of the MHE compared to the EKF in the presence of a poor initial SOC guess in the CCDT case.

5.2.2. DST case

For the DST profiles in the 10–100% SOC range, the estimation results based on the MHE and EKF with the correct initial SOC guess are shown in Fig. 8(a) and the corresponding AE profiles are shown in Fig. 8(b). For the MHE and EKF, the maximum AE values are 0.43% and 3.71% respectively, and the RMSE values are 0.15% and 1.36% respectively. These results show that although both methods could provide satisfied SOC estimation accuracy for real applications, the MHE performs better especially in the low SOC range, in which the OCV model usually has larger prediction errors. Compared to EKF, the AE profile of MHE appears much smaller fluctuations in the whole SOC range, indicating that the

MHE could provide a more stable and reliable SOC estimation. The main reason is that both previous and current measurements are used to update the arrival cost and simultaneously minimize the deviations of initial estimate, the battery dynamic model and output model in the MHE. The improved SOC estimation in the DST case suggests that the MHE is more suitable for the complex fast dynamic system.

To further verify the robustness of MHE in the variable power discharge condition, three DST cycles starting with 80%, 50% and 20% SOC are studied. Note that only one DST cycle of 360 s is used for performance evaluation. Two extreme poor initial SOC guesses, i.e. 100% and 0%, are used to investigate the effects of high and low initial guesses with respect to true SOC values on estimation performance. Fig. 9 show the SOC estimation and AE profiles of MHE and EKF with the initial SOC guess of 100% in the different cycles. For three DST cycles with 80%, 50% and 20% initial SOC, the first AE values of MHE are 0.55%, 2.16% and 2.98% respectively, while the first AE values of EKF is 6.36%, 21.33% and 41.94% respectively. Obviously, the MHE is able to achieve the true SOC much faster than EKF. It is also observed that the MHE slightly underestimates the SOC for the DST cycles with 80% and 50% initial SOC, and overestimates the SOC for the DST cycle with 20% initial SOC. Moreover, it can be found that the EKF shows obvious oscillation characteristics in both SOC estimation and AE profiles for all three DST cycles, which would produce unreliable and even confusing SOC estimates.

The estimation results of MHE and EKF with the initial SOC guess of 0% for three DST cycles are also compared in Fig. 10. For three DST cycles with 80%, 50% and 20% initial SOC, the first AE values of MHE are 0.44%, 1.29% and 2.30% respectively, while the first AE values of EKF are 69.11%, 41.96% and 14.27% respectively. Similar with Fig. 9, the results in Fig. 10 again demonstrate that the MHE could provide much faster and more reliable SOC estimates.

The RMSE comparison between MHE and EKF is shown in Table 5. The RMSE values of MHE are lower than that of EKF for all cases. The maximum RMSE value of MHE is only 1.88%, while that of EKF could reach up to 5.12%. For a certain DST cycle, the MHE is less sensitive to the given higher or lower initial SOC guess. In contrast, the EKF is much more sensitive to the initial guess value and direction, e.g. for the DST cycle with 80% initial SOC, the RMSE values obtained with the initial SOC guesses of 100% and 0% are 0.71% and 5.12% respectively. It implies that an arbitrary initial SOC guess might be chosen in MHE without sacrificing the estimation performance, which could significantly improve the ease use of MHE in real applications. To conclude, all these results demonstrate that the MHE can achieve more accurate and reliable SOC estimation for the DST cycles with different initial SOC.

6. Conclusion

In this work, a moving horizon estimation approach is proposed to estimate SOC based on a nonlinear battery state-space model, in which the relationships between SOC and circuit parameters are explicitly modeled by polynomial functions. Three characteristic tests at 293 K of a commercial LIB, i.e. HPPC, CCDT and DST, are used to validate the effectiveness of the proposed SOC estimation method. Based on the HPPC testing profile, the polynomial coefficients in battery model is estimated and both covariance matrices and horizon length in the MHE are optimally determined. It is found that the RMSE value of the constructed battery model is less than 10 mV and the SOC estimation RMSE value of MHE with optimal tuned parameters could reach below 1%. The CCDT and DST profiles are then used to systematically compare the SOC estimation performance between MHE and EKF with both correct and incorrect initial SOC guesses. For the CCDT case, it is found that (1) both MHE and EKF show comparable estimation performance when the correct initial SOC guess is used, and (2) the convergence to true SOC of MHE is faster than that of EKF when the incorrect initial SOC guess is used. For the DST case, when the correct initial SOC guess is used, the RMSE value of 0.15% using MHE is lower than that of 1.36% using EKF, and the MHE has fewer fluctuations than EKF. Moreover, three DST cycles with different initial SOC are used to further investigate the effect of lower and higher initial SOC guesses on the SOC estimation performance, and the faster and more reliable SOC estimate of MHE is again validated. Hence, these results show that the ECM-based MHE could provide a potential promising approach to perform accurate, reliable and robust SOC estimation.

Acknowledgments

The authors gratefully acknowledge financial support from the Major State Basic Research Development Program of China (2014CB239703), the National Natural Science Foundation of China (21576163, 21006084, 21336003), the Science and Technology Commission of Shanghai Municipality (14DZ2250800), and the Project-sponsored by SRF for ROCS, SEM.

References

Amrit R., Rawlings J.B., 2008. Nonlinear Model Predictive Control Tools (NMPC Tools). ⟨http://jbrwww.che.wisc.edu/software/mpctools/index.html⟩.
Charkhgard, M., Farrokhi, M., 2010. State-of-charge estimation for lithium-ion batteries using neural networks and EKF. IEEE Trans. Ind. Electron. 57, 4178–4187.
Chen, M., Rincon-Mora, G.A., 2006. Accurate electrical battery model capable of predicting runtime and I–V performance. IEEE Trans. Energy Convers. 21, 504–511.
Cheng, K.W.E., Divakar, B.P., Wu, H., Ding, K., Ho, H.F., 2011. Battery-Management System (BMS) and SOC development for electrical vehicles. IEEE Trans. Veh. Technol. 60, 76–88.
Chiasserini, C.F., Rao, R.R., 2001. Energy efficient battery management. IEEE J. Sel. Areas Commun. 19, 1235–1245.
Dey S., Ayalew B., 2014. Nonlinear Observer Designs for State-of-Charge Estimation of Lithium-Ion Batteries. pp. 248–253.
Doyle, M., Fuller, T.F., Newman, J., 1993. Modeling of galvanostatic charge and discharge of the lithium polymer insertion cell. J. Electrochem. Soc. 140, 1526–1533.
Erdinc O., Vural B., Uzunoglu M., 2009, A dynamic lithium-ion battery model considering the effects of temperature and capacity fading. In: Proceedings of the 2009 International Conference on Clean Electrical Power (Iccep 2009). vols. 1 and 2, pp. 374–377.
Findeisen R., Diehl M., Burner T., Allgower F., Bock H.G., Schloder J.P., 2002, Efficient output feedback nonlinear model predictive control. vol. 6, pp. 4752–4757.
Fleischer, C., Waag, W., Heyn, H.M., Sauer, D.U., 2014. On-line adaptive battery impedance parameter and state estimation considering physical principles in reduced order equivalent circuit battery models. J. Power Sources 260, 276–291.
Haseltine, E.L., Rawlings, J.B., 2005. Critical evaluation of extended kalman filtering and moving-horizon estimation. Ind. Eng. Chem. Res. 44, 2451–2460.
Hassoun, J., Scrosati, B., 2015. Review-advances in anode and electrolyte materials for the progress of lithium-ion and beyond lithium-ion batteries. J. Electrochem. Soc. 162, A2582–A2588.
He, H., Qin, H., Sun, X., Shui, Y., 2013a. Comparison study on the battery SOC estimation with EKF and UKF algorithms. Energies 6, 5088–5100.
He, W., Williard, N., Chen, C., Pecht, M., 2013b. State of charge estimation for electric vehicle batteries using unscented kalman filtering. Microelectron. Reliab. 53, 840–847.
He, Y., Shen, J., Shen, J., Ma, Z., 2015. Embedding monotonicity in the construction of polynomial open-circuit voltage model for lithium-ion batteries: a semi-infinite programming formulation approach. Ind. Eng. Chem. Res. 54, 3167–3174.
He, Y., Liu, X., Zhang, C., Chen, Z., 2013c. A new model for State-of-Charge (SOC) estimation for high-power Li-ion batteries. Appl. Energy 101, 808–814.
Hedengren J.D., Allsford K.V., Ramlal J., 2007. Moving Horizon Estimation and Control for an Industrial Gas Phase Polymerization Reactor. pp. 1353–1358.
Hu, X., Li, S., Peng, H., 2012. A comparative study of equivalent circuit models for Li-ion batteries. J. Power Sources 198, 359–367.
Hunt G., 2003. FreedomCAR Battery Test Manual For Power-Assist Hybrid Electric Vehicles. DOE/ID-11069.
Hunt, G., 1996. USABC Electric Vehicle Battery Test Procedures Manual. United States Department of Energy, Washington, DC, USA.

Jongerden, M.R., Haverkort, B.R., 2009. Which battery model to use? IET Softw. 3, 445–457.
Kühl, P., Diehl, M., Kraus, T., Schlöder, J.P., Bock, H.G., 2011. A real-time algorithm for moving horizon state and parameter estimation. Comput. Chem. Eng. 35, 71–83.
Kang, L., Zhao, X., Ma, J., 2014. A new neural network model for the state-of-charge estimation in the battery degradation process. Appl. Energy 121, 20–27.
Lee, S., Kim, J., Lee, J., Cho, B.H., 2008. State-of-charge and capacity estimation of lithium-ion battery using a new open-circuit voltage versus state-of-charge. J. Power Sources 185, 1367–1373.
Ma Y., Zhou X., Zhang J., 2014. Lithium-Ion Battery State of Charge Estimation Based on Moving Horizon. pp. 5002–5007.
Miranda, A.G., Hong, C.W., 2013. Integrated modeling for the cyclic behavior of high power Li-ion batteries under extended operating conditions. Appl. Energy 111, 681–689.
Ng, K.S., Moo, C.S., Chen, Y.P., Hsieh, Y.C., 2009. Enhanced coulomb counting method for estimating state-of-charge and state-of-health of lithium-ion batteries. Appl. Energy 86, 1506–1511.
Pattel B., Borhan H., Anwar S., 2014. An evaluation of the moving horizon estimation algorithm for online estimation of battery state of charge and state of health. In: Proceedings of the ASME 2014 International Mechanical Engineering Congress and Exposition. American Society of Mechanical Engineers. V04BT04A049-V04BT04A049.
Plett, G.L., 2004a. Extended Kalman filtering for battery management systems of LiPB-based HEV battery packs – Part 2. Modeling and identification. J. Power Sources 134, 262–276.
Plett, G.L., 2004b. Extended Kalman filtering for battery management systems of LiPB-based HEV battery packs – Part 3. State and parameter estimation. J. Power Sources 134, 277–292.
Plett, G.L., 2006. Sigma-point Kalman filtering for battery management systems of LiPB-based HEV battery packs. J. Power Sources 161, 1369–1384.
Rao, C.V., Rawlings, J.B., Lee, J.H., 2001. Constrained linear state estimation—a moving horizon approach. Automatica 37, 1619–1628.
Rao, C.V., Rawlings, J.B., Mayne, D.Q., 2003. Constrained state estimation for nonlinear discrete-time systems: stability and moving horizon approximations. IEEE Trans. Autom. Control 48, 246–258.
Rawlings, J.B., Ji, L., 2012. Optimization-based state estimation: current status and some new results. J. Process Control 22, 1439–1444.
Rezvanizaniani, S.M., Liu, Z.C., Chen, Y., Lee, J., 2014. Review and recent advances in battery health monitoring and prognostics technologies for electric vehicle (EV) safety and mobility. J. Power Sources 256, 110–124.
Russo L.P., Young R.E., 1999. Moving-Horizon State Estimation Applied to an Industrial Polymerization Process. vol. 2, pp. 1129–1133.
Salkind, A.J., Fennie, C., Singh, P., Atwater, T., Reisner, D.E., 1999. Determination of state-of-charge and state-of-health of batteries by fuzzy logic methodology. J. Power Sources 80, 293–300.
Seaman, A., Dao, T.S., McPhee, J., 2014. A survey of mathematics-based equivalent-circuit and electrochemical battery models for hybrid and electric vehicle simulation. J. Power Sources 256, 410–423.
Shen, J., He, Y., Ma, Z., 2016. Simultaneous model selection and parameter estimation for lithium-ion batteries: a sequential MINLP solution approach. AIChE J. 62, 78–89.
Sun, F., Hu, X., Zou, Y., Li, S., 2011. Adaptive unscented Kalman filtering for state of charge estimation of a lithium-ion battery for electric vehicles. Energy 36, 3531–3540.
Xing, Y., He, W., Pecht, M., Tsui, K.L., 2014. State of charge estimation of lithium-ion batteries using the open-circuit voltage at various ambient temperatures. Appl. Energy 113, 106–115.
Yang, F., Xing, Y., Wang, D., Tsui, K.L., 2016. A comparative study of three model-based algorithms for estimating state-of-charge of lithium-ion batteries under a new combined dynamic loading profile. Appl. Energy 164, 387–399.
Zavala, V.M., Biegler, L.T., 2009. Optimization-based strategies for the operation of low-density polyethylene tubular reactors: moving horizon estimation. Comput. Chem. Eng. 33, 379–390.